RESEARCH ARTICLE

A Comprehensive Observation of the Morphology and the Neurovascular Pattern of the Triangular Fibrocartilage Complex [TFCC] of the Wrist Joint

Nandini Rajaram, MD; Dinesh Kumar V., MD

Research performed at Jawaharlal Institute of Postgraduate Medical Education and Research, Puducherry
Received: 25 November 2024

Accepted: 12 April 2025

Abstract

Objectives: This study aims to provide a comprehensive understanding of the unique morphological dimensions and neurovascular pattern of the triangular fibrocartilage complex (TFCC) of the wrist joint, using innovative techniques such as digital Vernier calliper, auramine chloride (Palmgren's method) and immunohistochemistry.

Methods: Samples were collected from 20 formalin-embalmed human cadavers. The morphometric parameters were measured. After gross examination, tissues were placed in 10% neutral buffered formalin for fixation. Paraffinembedded blocks were prepared, and tissue sections were taken at 5-7 microns thickness. The slides were subjected to Palmgren's and immunohistochemistry staining following a standardised protocol.

Results: The morphometric parameters of the articular disc (AD) and neurovascular pattern of the seven components of TFCC were assessed. There was no significant difference in the morphometric parameters between either sides of the limb. The AD had minimal nerve fibre innervation. Periphery of the complex, which consisted of different ligaments, showed higher nerve density comparatively. The distribution of nerve fibres predominated in the proximal portion compared to distal areas of TFCC. The vascular pattern observed in various components showed fewer blood vessels in the AD than in the periphery. Higher vascularity was observed in the proximal portion of the TFCC complex.

Conclusion: The insights gained from this study, particularly the understanding of the innervation and distribution of nerve fibres of TFCC, can significantly enhance the effectiveness of selective denervation procedures during wrist arthroscopy. Moreover, the knowledge about the vascularity of TFCC is a crucial factor that can influence the end outcomes of wrist surgeries.

Level of evidence: IV

Keywords: Neurovascular pattern, Triangular fibrocartilage complex, Wrist joint

Introduction

The wrist joint is a complex joint with many movements.¹ The triangular fibrocartilage complex (TFCC) is one of the critical structures to maintain stability and facilitate the functional performance of the joint.² The complex anatomy of the ulnar side of the wrist offers excellent challenges in understanding, diagnosing and treating its pathologies. The complex nature of this structure makes it difficult to arrive at a consensus in the management of pathologies in this joint. Ulnar wrist pain is

one of the most common wrist problems perceived by hand surgeons. It may be acute or chronic and includes the following causes: fractures, dislocations, ligament injuries, avascular necrosis, and degenerative changes affecting the ulnar carpus and distal radioulnar joint. In the elderly groups, wrist pain has been emerging as an essential treatment modality, making the entire focus on the wrist joint. It has been noted that TFCC remains the most recognised cause of ulnar wrist pain.³ This urges us to

Corresponding Author: Dinesh Kumar V., Department of Anatomy, Jawaharlal, Institute of Postgraduate Medical Education and Research, Puducherry, India

ABS THE ONLINE VERSION OF THIS ARTICLE ABJS.MUMS.AC.IR

Arch Bone Jt Surg. 2025;13(11):711-719 Doi: 10.22038/ABJS.2025.84143.3824 http://abjs.mums.ac.ir



Email: dinesh.88560@gmail.com

analyse the complex anatomical and biomechanical structure of TFCC.

The triangular fibrocartilage complex (TFCC) is a complicated ligamentous fibrocartilaginous structure composed of multiple anatomical structures located in the ulnar aspect of the human wrist separating the radiocarpal and distal radioulnar joints. TFCC has seven distinct components: "the articular disc (AD), the volar radioulnar ligament (VRUL), the dorsal radioulnar ligament (DRUL), the ulno lunate (UL), the ulno triquetral ligaments (UT q), the sub sheath of the extensor carpi ulnaris (SS-ECU) tendon and the ulnocarpal meniscoid structure (UCM).4 Extra-articular tissues, especially nerves and tendons, are at risk during wrist arthroscopy.⁵ The wrist joint is densely innervated by neurons, especially mechanoreceptors, to high-quality proprioceptive functions. perform pathologies involving the wrist joint result in significant pain owing to the intense neuronal innervation in the form of free nerve endings.⁶ Recent studies point that posterior cutaneous branch of ulnar nerve, medial cutaneous branch of forearm and palmar sensory branch of ulnar nerve provide innervation to the TFCC structure. Studies on these innervations is very vital as wrist pain on the ulnar aspect is often observed following degenerative or traumatic pathologies affecting the wrist joint. The mechanism of chronic wrist pain and the sensation of wrist instability can be studied by observing the distribution pattern of mechanoreceptors in TFCC. Further these data on neural innervation of TFCC can facilitate disc replacement surgery for TFCC in future for wrist joint pathologies. The highly vascularised structures of TFCC are likely to heal better than less vascularised structures. The complication rates of arthroscopic procedures will be better in future when the position of portals are performed in structures which are more likely to heal better.⁷ Hence, studying the vascular distribution pattern can facilitate surgical planning and provide insight into the suturing pattern, thereby preventing degeneration.

The anatomy of TFCC has not been extensively studied in the Indian population, especially the pattern of neurovascular distribution. This study aimed to describe the neurovascular pattern of the triangular fibrocartilage complex of the wrist joint using auramine chloride staining (Palmgren's method) and immunohistochemistry.

Materials and Methods

This study was conducted in a total of 40 upper limbs from 20 formalin embalmed cadavers of either sex. The Institutional Ethics Committee granted a waiver of consent. The embalmed cadavers that were found suitable for dissection during the study duration were included in the study. Cadavers with obvious pathological, traumatic, or degenerative abnormalities in the wrist joint region were excluded from the study. Dissection of the wrist joint was performed using a transverse incision across the front of the wrist joint. The annular ligament was cut, and the interosseus membrane was divided downward from above. The Radius bone was drawn laterally to expose the connections of the articular capsule and disc [Figure 1]. The structural complex of fibrocartilage and its associated structures was detached proximally using an oblique osteotomy of the ulnar head, proximal to the fovea and ulnar styloid. Following the direction of the most proximal fibres of the dorsal radio triquetral ligament, a dorsal radiocarpal capsulotomy was used to enter the TFCC. After sectioning the soft tissues and capsule of the distal radioulnar joint, TFCC was removed [Figure 1]. Upon exposure to the TFCC complex, the morphometric parameters such as length and width at the proximal and distal attachment, width at the centre, and length and width of associated structures in prone and supine positions of the forearm will be measured and documented. A single investigator will take the measurements of morphometric parameters to the nearest millimetres using a digital Vernier calliper [Figure 1]. After gross examination, TFCC was kept in 10% neutral buffered formalin for two days for fixation. All specimens were then embedded in paraffin. Two transverse slices of approximately 0.5 cm thickness were taken (the first slice from the proximal attachment and the second slice from the distal attachment). On tissue processing, 5- 7 µm thick sections were prepared. The tissue samples were washed with normal saline and transferred to the tissue cassettes for tissue processing, followed by tissue sectioning.

Palmgren's silver staining method

Sections were deparaffinised and hydrated. Slides were placed into acid formalin. Slides were rinsed with distilled water and transferred to silver solution. Slides were drained, subjected to a reducing solution, and then rinsed with 50% alcohol. Slides were again rinsed, toned with gold chloride, and transferred to an intensifier. Slides were then fixed with a fixing bath solution containing 5% sodium thiosulphate. Slides were rinsed, well dehydrated, cleared, and then mounted by DPX.

Immunohistochemistry-Immunofluorescent method

Deparaffinisation and hydration of the tissue section were done on the first day. Antigen retrieval is done with antigen retrieval buffer using the pressure cooker method. The slides were changed to wash buffer and then emptied from the slide, and 50-100 μl of blocking buffer was added and incubated in a moist chamber for 45 minutes. The diluted primary antibody (Anti-VE cadherin) of $100\mu l$ with 1/1000 was added and incubated in the fridge overnight.

On the second day, the slides were rinsed with chilled wash buffer. The diluted secondary antibody (Cy 5) of 100 μ l with 1/500 concentration was added in a dark room to prevent auto bleaching and then incubated for 60 mins. The slides were treated with chilled wash buffer and 1x PBS. Counter-staining was done with DAPI. Slides were rinsed with 1X PBS mounted using fluoromount aqueous medium, and the edges of the coverslip were sealed with nail polish.

Morphometric parameters, such as length, width, and area of TFCC's articular disc near its proximal and distal attachment, were observed using digital Vernier callipers (Mitutoyo, Tokyo, Japan). The slides were examined using the bright field compound microscope (Olympus CX41, Tokyo, Japan) under 4X, 10X and 40X magnification, and pictures were taken with a digital camera fitted into a microscope for Palmgren's staining. A confocal microscope (Carl Zeiss LSM 700, Germany) was used for the slide examination, and the Zen software version 2010 was used create microscopic images the immunohistochemistry-immunofluorescent method. Positive reactions for blood vessels were detected as red

NEUROVASCULAR DEMONSTRATION OF TFCC OF THE WRIST JOINT

fluorescence, respectively. The images were taken and stored in the software. The software adjusted the imaging parameters such as objective lens, filter sets, and acquisition speed. Data for luminal area measurements were calculated using Image J software.

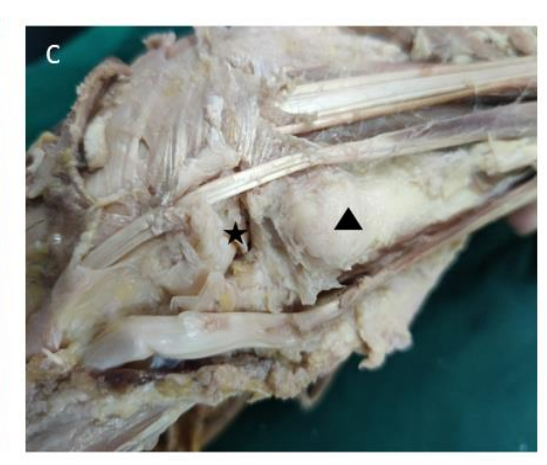
Statistical analysis

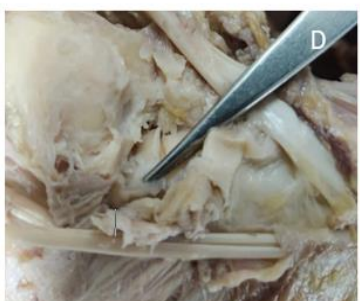
The results of morphometric, auramine chloride staining parameters of the cadaveric study were

expressed as frequencies/ proportions for nominal variables and mean with standard deviation or median with range for continuous variables. The data regarding proximal and distal parts of parameters were compared: Continuous variables were compared using an independent t-test/Mann-Whitney U test, and Nominal variables were compared using the Chi-Square test, whichever is applicable. P <0.05 will be considered as statistically significant.













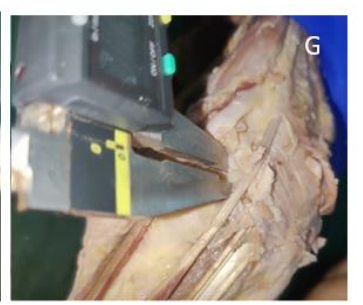


Figure 1. Ulnar aspect of left wrist joint showing the gross structure of triangular fibrocartilage complex. (A & B) Gross image of ulnar side of the Left wrist joint. (C) The articular disc complex of triangular fibrocartilage complex of the left wrist joint. Black triangle points the ulnar styloid process and black asterix demonstrates triangular fibrocartilage complex (D) The articular disc along with the entire complex of the triangular fibrocartilage of the left wrist joint. Morphometric evaluation of (E) length and (F) breadth of the articular disc using digital vernier caliper (Mitutoyo brand) of the left wrist joint (G) The cut ends of proximal and distal portion of triangular fibrocartilage complex of the left wrist joint

Results

A total of 40 wrist joints were utilised for the study. Of these, 50% were in the right upper limb, and the rest, 50% were in the left upper limb. The limbs were subjected to dissection steps as detailed in the methodology section, and details of the TFCC structure were collected. The neurovascular pattern of all seven components of TFCC was studied and compared between the right and left sides and the proximal and distal parts of TFCC. The morphometric details of the articular disc are presented [Table 1]. The distribution of nerve fibres is given [Table 2]. The details of distribution of blood vessels are presented [Table 3, 4].

Morphometry details of articular disc

The range of length, breadth and area of the articular disc were 6.62 to 9.11 mm, 3.97 to 5.21mm and 20.78 to 41.95mm², respectively, on the right side. The articular disc's length, breadth and area were 6.16 to 9.47 mm, 3.73 to 5.63mm and 20.69 to 43.16mm² respectively, on the left side. The median length, breadth, and location are shown [Table 1]. There was no significant difference in the above parameters between either sides of the limb.

NEUROVASCULAR DEMONSTRATION OF TFCC OF THE WRIST JOINT

Table 1. Morphometric evaluation of triangular fibrocartilage complex of wrist joint								
Morphometry parameter	Side	Observation (median [IQR])	P value					
Length (mm)	Right side	7.8 (6.71, 8.61)	0.64					
	Left side	7.54 (6.91, 8.52	0.61					
Breadth (mm)	Right side	4.21 (3.82, 4.98)	0.51					
	Left side	4.33 (3.71, 5.11)						
Area (mm²)	Right side	28.65 (21.2, 39.76)	0.69					
	Left side	29.12 (22.1, 41.56)						

Table 2. Number of nerve fibres in different components of Triangular Fibrocartilage complex										
	Number of nerve fibres									
Structure of TFCC		Proximal		Distal						
	Right	Left	P value	Right	left	P value				
Articular disc	1.65 ± 0.67	2.35 ± 1.18	0.19	2.35 ± 1.18	2.1 ± 0.78	0.92				
Volar radio-ulnar ligament	6.55 ± 1.94	6.15 ± 0.87	0.76	4.97 ± 0.85	5.05 ± 0.99	0.88				
Dorsal radio-ulnar ligament	6.05 ± 0.82	6.35 ± 0.98	0.91	6.55 ± 0.82	6.05 ± 0.88	0.93				
Ulno-lunate ligament	17.89 ± 1.79	17.42 ± 2.36	0.87	15.42 ± 1.21	16.31 ± 2.38	0.91				
Ulno-carpal meniscoid	18.26 ± 2.22	18.52 ± 2.64	0.86	15.64 ± 1.82	15.85 ± 2.81	0.79				
Ulno-triquetral ligament	18.05 ± 2.57	18.52 ± 2.82	0.92	15.26 ± 2.26	15.6 ± 2.11	0.84				
Sub-sheath of extensor carpi ulnaris tendon	19.23 ± 2.38	19.1 ± 2.74	0.86	15.99 ± 2.44	15.31 ± 3.13	0.81				

Table 3. Number of blood vessels in components of Triangular Fibrocartilage complex										
	Blood vessels									
	Proximal				Distal					
Components of Triangular fibro-cartilage complex		Right		Left		Rig	Right		eft	
		Proportion of cadavers (%)	Number of vessels	Proportion of cadaver (%)	P value	Number of vessels (%)	Proportion of cadavers (%)	Number of vessels (%)	Proportion of cadavers (%)	P value
Articular disc	0 1	65 35	0 1	60 40	0.62	0 1	60 40	0 1	65 35	0.42
Volar radio-ulnar ligament	1 2 3	30 45 25	1 2 3	40 35 25	0.73	1 2 3	40 40 20	1 2 3	40 45 15	0.74
Dorsal radio-ulnar ligament		15 55 30	1 2 3	35 50 15	0.64	1 2 3	45 45 10	1 2 3	45 40 15	0.79
Ulno-lunate ligament	3 4 5	40 50 10	3 4 5	25 50 25	0.73	3 4 5	50 40 10	3 4 5	35 50 15	0.71
Ulno-carpal meniscoid	3 4 5 6	25 45 5 5	3 4 5 6	20 40 25 15	0.73	3 4 5 6	20 35 25 15	3 4 5 6	25 45 20 10	0.71

NEUROVASCULAR DEMONSTRATION OF TFCC OF THE WRIST JOINT

Table 3. Continued										
Ulno-triquetral ligament	5 6 7 8	10 20 55 15	5 6 7 8	15 15 30 40	0.61	5 6 7 8	15 45 25 15	5 6 7 8	15 20 55 10	0.77
Sub-sheath of extensor carpi ulnaris tendon	6 7 8 9	10 15 30 45	6 7 8 9	10 10 40 40	0.88	6 7 8 9	15 20 35 30	6 7 8 9	15 20 40 25	0.81

ble 4. Surface area of blood vessels in components of Triangular Fibrocartilage complex											
	Surface area of blood vessels (µm²)										
Structure of Triangular Fibrocartilage complex		Proximal	Distal								
The court sauge complem	Right	Left	P value	Right	left	P value					
Articular disc	889 (834, 1403)	869 (802, 1654)	0.69	985 (902, 1430)	873 (812, 1327)	0.32					
Volar radio-ulnar ligament	3662 (2891, 4972)	3519 (2761, 4592)	0.79	3673 (2761, 4672)	3768 (2633, 4251)	0.71					
Dorsal radio-ulnar ligament	3590 (2963, 5897)	3871 (2961, 5602)	0.67	3292 (2569, 5241)	3791 (2426, 5015)	0.58					
Ulno-lunate ligament	6927 (5099, 8920)	6726 (5345, 8876)	0.86	7452 (4998, 8475)	7108 (4692, 8762)	0.24					
Ulno-carpal meniscoid	8778 (6709, 9012)	8029 (7238, 9282)	0.79	8383 (6746, 8673)	8019 (7060, 9281)	0.74					
Ulno-triquetral ligament	10045 (8209, 14034)	10298 (8401, 15621)	0.84	11362 (8812, 14399)	11762 (8945, 14876)	0.72					
Sub-sheath of extensor carpi ulnaris tendon	12619 (10191, 16465)	12934 (10091, 16783)	0.86	12843 (10068, 16743)	13394 (10934, 17217)	0.93					

Articular disc

Nerve fibres were sparse and few in the articular disc (AD) and neural distribution is presented [Table 2]. There was no difference in its distribution between either sides or between the proximal and distal parts of TFCC [Figure 2]. Blood vessels were few in AD and vascular distribution is presented [Table 3]. The surface area of blood vessels in the proximal part of AD by immunohistochemistry was in the range of 799 to $1510 \, \mu m^2$ on the right side and 776 to 1710 on the left side [Table 4]. There was no difference between the surface area of blood vessels between either side limb and the proximal and distal part of AD [Figure 3].

Volar Radio-ulnar ligament

The distribution of nerve fibres was not significantly different between either side and between the proximal and distal parts of the Volar Radio-ulnar ligament (VRUL). Blood vessels were in the range of 1 to 3 on both sides. There was no difference in the number of blood vessels and surface area of blood vessels between either side and between the proximal and distal parts of VRUL.

Dorsal radio-ulnar ligament

The number of nerve fibres in the distal part of the dorsal radio-ulnar ligament (DRUL) detected by auramine chloride stain was in the range of 5 to 8 on the right side and 5 to 8 on the left side [Figure 2]. There was no significant difference between the number of nerve fibres, blood vessels and surface area of blood vessels on either side of the limb and

between the proximal and distal parts of DRUL.

Ulno-lunate ligament

The number of nerve fibres in the proximal part of the Alnolunate ligament (UL) detected by auramine chloride stain ranged from 15 to 22 on the right side and 14 to 22 on the left side. There was no significant difference in the number of nerve fibres between the proximal and distal parts of UL. The number of blood vessels in the proximal part of UL ranged from 3 to 5 on the right side and 3 to 5 on the left side. There was no significant difference between the number and surface area of blood vessels in tissues from either side of the limb and proximal and distal parts of UL.

Ulnocarpal meniscoid

The number of nerve fibres in the proximal part of ulnocarpal meniscoid (UCM) detected by auramine chloride stain was in the range of 15 to 23 on the right side and 15 to 24 on the left side. The number of blood vessels in the proximal part of UCM ranged from 3 to 6 in the right side and 3 to 6 in the left side. There was no significant difference between the number of nerve fibres and blood vessels in tissues from either side of the limb and the proximal and distal parts of UCM.

Uno-triquetral ligament

The number of nerve fibres, blood vessels, and surface area of blood vessels were similar between either side and the proximal and distal part of ulno-triquetral ligament (UTL).

NEUROVASCULAR DEMONSTRATION OF TFCC OF THE WRIST JOINT

Sub-sheath of extensor carpi ulnaris tendon

The number of nerve fibres and blood vessels and surface area of blood vessels were similar between either side as well

as between the proximal and distal part of the Sub-sheath of extensor carpi ulnaris (SSECU) tendon.

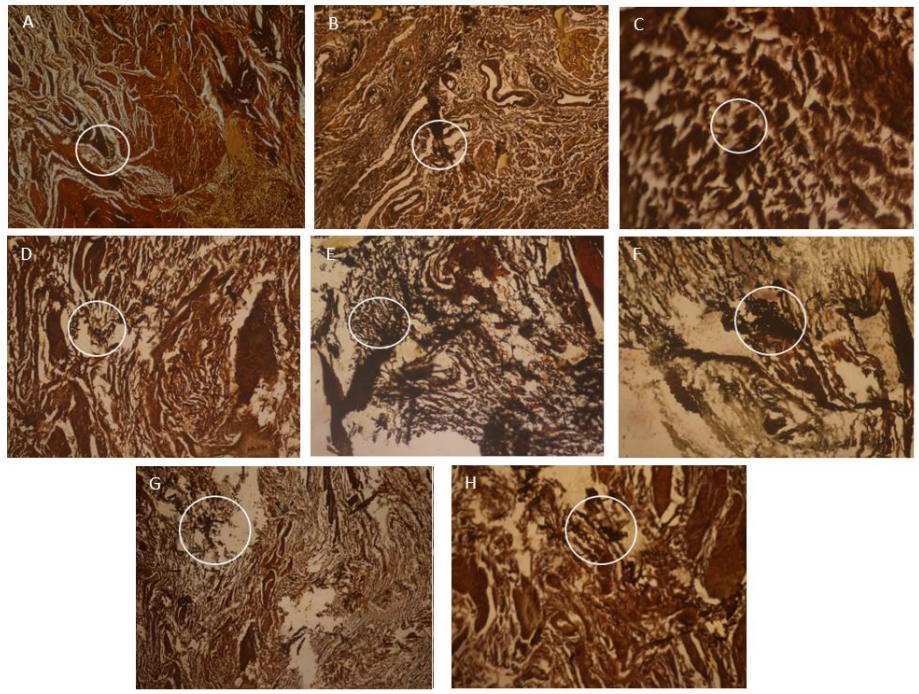


Figure 2. Auramine chloride (Palmgren's method) staining where white circles demonstrate the distribution of nerve fibers. Transverse section of proximal part of articular disc in different magnifications (A)-4x, (B)-10X, (C)-40X. Transverse section of distal part of triangular fibrocartilage complex in different magnifications (D)-4x, (E) -10X, (F)-40X. Transverse section of distal part of epi ligament (Dorsal radioulnar ligament) (G)-4x (H) -10X

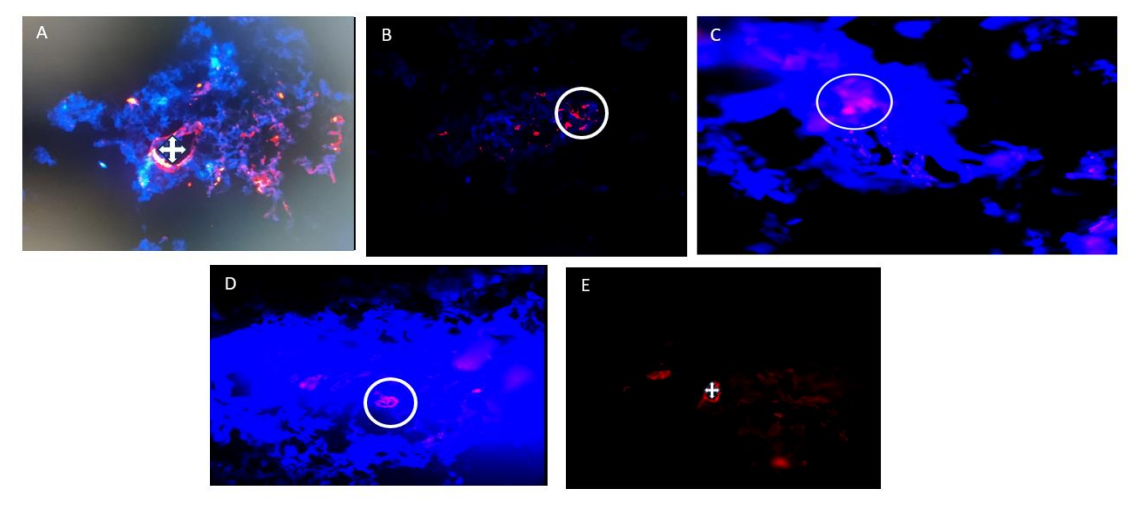


Figure 3. Immunohistochemical staining demonstrating the blood vessels in white circles. Proximal part of triangular fibrocartilage complex in various fields using immunohistochemistry-immunofluorescence method. (A) White arrow demonstrates the measurement of luminal area of blood vessel. (B & C) White circles demonstrates blood vessel .Stain: Nuclei: DAPI; Endothelium: VE cadherin primary antibody; Cy-5 tagged secondary antibody. Distal part of triangular fibrocartilage complex using immunohistochemistry-immunofluorescence method in different fields. (E) White circle shows blood vessel and (E) White arrow displays the measurement of luminal area of blood vessel. Stain: Nuclei: DAPI; Endothelium: VE cadherin primary antibody; Cy-5 tagged secondary antibody

Discussion

It was known that TFCC comprises a central fibrocartilaginous disc and surrounding fibro-ligamentous

structures. ^{1,8-16} In the present study, we observed that neural density was minimal in the articular disc area compared to the periphery of the TFCC. Nerve fibres in other components

of TFCC predominated. Avascularity was observed in the central portion of the articular disc area compared to the periphery. The other ligamentous structures showed increased vascularity comparatively. Similar findings was observed in study by Kirchberger et al.¹⁷

Articular disc

The articular disc showed sparse vascularity compared to other peripheral areas of the TFCC in our study. Avascularity was seen in central and the radial regions compared to the disc's ulnar border, which showed sparse vascularity. The articular disc's central area showed the least nerve fibres. The one study showed that the articular disc area was not innervated. Another study also showed avascularity in the inner portion of the disc. A similar pattern of avascularity had been reported in the central portion of the disc and its radial attachment. In his classification, Palmer also showed that any avulsions or tears in the central area of TFCC were not showing a reparative response due to less blood supply in this region.

Volar radioulnar ligament (VRUL) and Dorsal Radioulnar ligament (DRUL)

The vascularity of these epi-ligaments was comparatively higher near the volar and dorsal margins than near the margins contiguous to the disc.^{12,16} The epi ligaments (VRUL and DRUL) showed increased neural density compared to the articular disc, similar to one study's findings.¹⁹ Their study found an increased number of nerve fibres in these areas. The distribution of nerve fibres in the dorsal and radial regions of TFCC implies their central role in proprioceptive function.²⁰ These radioulnar ligaments act as primary stabilisers of the distal radioulnar joint. All types of mechanoreceptors and sensory nerve endings have been found in these ligaments, and it has been postulated that these ligaments help in joint position change, and their richer innervation plays a vital role in neuromuscular stability.²¹ Palmer's classification described the rich vascular supply in these regions of TFCC and showed that the healing potential was better after repairs of TFCC.²⁰ One study showed similar observation regarding increased vascularity in these ligaments and their role in repairing TFCC tears.¹⁹ The capillary plexus from the radioulnar ligaments had innervated the peripheral 10 to 15 % of the articular disc. VRUL had an essential role in detecting joint position change due to the presence of more Ruffini nerve endings.²² Proprioceptive exercises had been recommended for better ligament healing after the reattachment of VRUL and DRUL in the postoperative follow-up.²³

Ulno-lunate ligament

This ligament had little vascularity. The number of nerve fibres was little increased compared to the central portion of the disc area in our study, which corresponded to an earlier study. Ulno-lunate ligament, similar to the articular disc, was an exception since it did not contain all types of sensory corpuscles, whereas sensory nerve endings and some Golgi corpuscles were seen in ulno-lunate ligament in their study. The classification of specific sensory nerve endings according

to neurophysiology and morphological traits of each ligament was reported.²⁴ Thus, some sensory nerve endings and Golgi corpuscles point out that the ulno lunate ligament implications mainly in mechanical functions and the sensory nerve endings perceive noxious, inflammatory and chemical stimuli. On the contrary, one study pointed out that only the central part of the disc was not innervated, but all the areas in the periphery showed innervation.⁶ The presence of blood vessels was lesser compared to the volar radioulnar ligament, but vascularity was present in comparison to the articular disc, which was avascular in our current study, and these findings correlated with the findings conducted in a study.²¹ Other studies also proved the presence of arterial supply in their experiments. The recent research on surgical repair of peripheral tears of TFCC conducted on 11 patients mounted a response with normal and painless activities after follow-up, which reveals that peripheral areas of TFCC had better healing potential due to rich vascular supply.²⁵

Ulno-triqueteral ligament

The vascularity was comparatively higher than that of the ulno-lunate ligament, and the fascicular and epifascicular regions both showed higher vascularity. This ligament had a higher distribution of nerve fibres, a finding similar to our present study. All types of sensory nerve corpuscles were found in this ligament, as appreciated by one study. It was pointed out that this ligament in the periphery of TFCC showed innervation. Thus, this ligament plays a role in proprioceptive function, thereby indirectly responsible for the neuromuscular and distal radioulnar joint stability. The vascularity was noted to be higher in their experiments. This pattern of vascularity has been helpful in the classification of TFCC tears and the healing of surgical repairs of TFCC tears.

Ulnocarpal-meniscoid

There was rich vascularity in this ligament, which points towards the structure's good healing ability.²⁴ Free nerve endings had been found uniformly distributed throughout the components of TFCC.²⁶ The ulnocarpal meniscoid showed more significant innervation than the disc and ulnolunate ligaments in our study, and the same results were obtained in one study.²⁷ It has been demonstrated that this component of TFCC showed increased innervation and revealed all types of mechanoreceptors to be present, as well as their role in nociception and maintaining the distal radioulnar joint stability.²¹ In most of the cases, the meniscus had free nerve endings without the presence of myelin. The axons of the meniscus were present with Schwann cells, and the bulb endings like Meissners's corpuscules and Krause's corpuscles were noted in this area. These articular corpuscles helped function with position, movement, and vibration sensation. Also, some sensory corpuscles like Golgilike, Pacini, Ruffini, and unclassifiable corpuscles were observed in them.²⁸ They had a good amount of vascularisation, as shown in the current study, and they matched with the findings of Rein et al.²¹ The healing potential of the meniscus was proved in a dog experiment in which an incision given in the vascularised area of the meniscus showed the potential for repair in their study.²⁹

The similar biological nature of the meniscus and TFCC helped draw the conclusion that the repair response was based on which tear pattern.

Sub sheath of extensor carpi ulnaris tendon

Blood vessels were predominant at the insertion sites. In the present study, there was a more excellent distribution in the number of nerve fibres, and the findings were similar to those of fewer studies.^{6,19} All sensory nerve corpuscles were found to be distributed in this sub-sheath, and their role in proprioceptive function has been emphasised. The vascularity was good in the current study, which correlated with the finding that peripheral areas of the disc had a rich supply. The peripheral area, 10 to 40% of the disc area, showed increased vascularity, which was confirmed in the present study. Palmer had classified this sub-sheath as the type of lesion that heals better due to a good amount of vascular supply.²²

Knowledge regarding the anatomy of TFCC shall be highly yielding for arthroscopic surgeons planning surgeries involving the wrist joint. Consequently, diminished rates of structural injury and better reconstruction of wrist joints are expected to be achieved. It is also helpful for radiologists to interpret scans of patients presenting with chronic wrist pain. This study provides a detailed analysis of the neurovascular pattern of TFCC. This analysis is expected to benefit the operating surgeons and patients by preventing complications like structural injury and avascular degeneration during arthroscopic procedures. Injury to the dorsal sensory branch of the ulnar nerve, the sensory branch of the radial nerve, the posterior interosseous nerve and extensor tendons can be prevented during the surgical procedure if the exact anatomical pattern and variations of TFCC are studied. By understanding the neurovascular pattern, the repair of TFCC tears can be made in a better way to yield better surgical outcomes and better reconstruction of the wrist joint. It is also helpful for radiologists to interpret scans of patients presenting with chronic wrist pain.

Conclusion

The central component of TFCC were sparsely peripheral vascularised than components epiligaments were richly innervated than articular disc. The articular disc area of TFCC showed minor nerve fibre distribution and avascularity except in the peripheral portion of the disc. The epi ligaments, especially the volar showed increased neuronal radioulnar ligament, distribution and a better amount of arterial supply than the dorsal radioulnar ligament. The other components of TFCC, like the ulno triquetral ligament, ulnocarpal meniscoid, and sub sheath of extensor carpi ulnaris tendon, showed an increased number of nerve fibres, and the vascular pattern was good enough except the ulno lunate ligament. This ulno lunate ligament rarely showed neuronal and vascular innervation. Thus, this neurovascular arrangement will be of immense help in the classification of TFCC tears and their surgical repairs. The anatomy of TFCC hasn't been extensively studied in the Indian population. Even though the salience of studying the anatomy of TFCC has been well realised in the past decade, the available literature remains scarce. Hence, the study has been formulated, and the outcomes of the study will serve as much-needed data while planning arthroscopic procedures and relevant radiological observations. Avascular degeneration and nerve injury in TFCC can possibly be prevented with an unfathomable understanding of the pattern of vasculature and free nerve endings. With the availability of the techniques mentioned above, we could study the anatomy of TFCC in a more lucid way than ever before.

The neurovascular pattern of the components of triangular fibrocartilage complexes was assessed. The articular disc consisted of the most minor nerve fibres, and the periphery of the complex, which consisted of the different ligaments, showed higher nerve density comparatively. The distribution of nerve fibres predominated in the proximal portion compared to distal areas of TFCC. The vascular pattern observed in various components showed fewer blood vessels in the articular disc than in the periphery. Higher vascularity was observed in the proximal portion of the TFCC complex. Analysing the innervation and distribution of nerve fibres of TFCC will be of immense help in selective denervation procedures during wrist arthroscopy. Knowledge regarding the vascularity of TFCC is a crucial factor for determining the end outcomes of wrist surgeries. With the observations from our study highly vascularised regions must be utilised for portal placement during arthroscopic procedures to permit faster healing and epiligament related pathologies are more likely to be painful than the pathologies affecting articular disc.

Acknowledgement

Dr. M Prabhu and Mrs. Kasturi, Department of Pathology, JIPMER, Puducherry for their support in performing the immunohistochemical evaluation of the specimen.

Authors Contribution: NR collected the data, reviewed the literature and drafted the manuscript. NR performed the data analysis. DKV conceptualised the study and critically revised the manuscript. All authors contributed to review of literature, drafting of the manuscript and approved the final version of the manuscript. DKV shall act as guarantor of the paper.

Declaration of Conflict of Interest: The authors declare no conflict of interests.

Declaration of Funding: The study was funded by the intramural grant sanctioned by the Institution, JIPMER, Puducherry.

Declaration of Ethical Approval for Study: The study was approved by the Institutional ethics committee for observational studies and certificate number JIP/IEC/320/2021 dated 22.02.2021

Declaration of Informed Consent: The data that support the findings of this study are available from the corresponding author upon reasonable request.

Nandini Rajaram MD ¹ Dinesh Kumar V. MD ¹

1 Department of Anatomy, Junior Resident, Jawaharlal Institute of Postgraduate Medical Education and Research, Puducherry, India

References

- Nakamura T, Matsumura N, Iwamoto T, Sato K, Toyama Y. Arthroscopy of the distal radioulnar joint. Handchir Mikrochir Plast Chir. 2014;46(5):295-9. doi: 10.1055/s-0034-1387706.
- 2. Ishii S, Palmer AK, Werner FW, Short WH, Fortino MD. An anatomic study of the ligamentous structure of the triangular fibrocartilage complex. J Hand Surg Am. 1998;23(6):977-85. doi: 10.1016/S0363-5023(98)80003-8.
- 3. Watanabe A, Souza F, Vezeridis PS, Blazar P, Yoshioka H. Ulnar-sided wrist pain. II. Clinical imaging and treatment. Skeletal Radiol. 2010;39(9):837-57. doi: 10.1007/s00256-009-0842-3.
- Skalski MR, White EA, Patel DB, Schein AJ, RiveraMelo H, Matcuk GR Jr. The Traumatized TFCC: An Illustrated Review of the Anatomy and Injury Patterns of the Triangular Fibrocartilage Complex. Curr Probl Diagn Radiol. 2016;45(1):39-50. doi: 10.1067/j.cpradiol.2015.05.004.
- 5. Lee SJ, Bae DS. Triangular Fibrocartilage Complex Injuries in Children and Adolescents. Hand Clin. 2021;37(4):517-526. doi: 10.1016/j.hcl.2021.06.004.
- 6. Cavalcante ML, Rodrigues CJ, Mattar R Jr. Mechanoreceptors and nerve endings of the triangular fibrocartilage in the human wrist. J Hand Surg Am. 2004;29(3):432-5. doi: 10.1016/j.jhsa.2004.01.001.
- 7. Tiburzi H, Machado CAG, D'Antoni MS, Tubbs RS. Triangular Fibrocartilage Complex: An Anatomical and Medical Illustration Study. Clin Anat. 2025;38:362-69. doi: 10.1002/ca.24261.
- 8. Chidgey LK. Histologic anatomy of the triangular fibrocartilage. Hand Clin. 1991;7(2):249-62
- Benjamin M, Evans EJ, Pemberton DJ. Histological studies on the triangular fibrocartilage complex of the wrist. J Anat. 1990; 172:59-67.
- 10. Nakamura T, Yabe Y, Horiuchi Y. Functional anatomy of the triangular fibrocartilage complex. J Hand Surg Br. 1996;21(5):581-6. doi: 10.1016/s0266-7681(96)80135-5.
- 11. Palmer AK, Werner FW. The triangular fibrocartilage complex of the wrist--anatomy and function. J Hand Surg Am. 1981;6(2):153-62. doi: 10.1016/s0363-5023(81)80170-0.
- 12. Mikic ZD. Treatment of acute triangular fibrocartilage complex injuries associated with distal radioulnar joint instability. J Hand Surg Am. 1995;20(2):319-23. doi: 10.1016/S0363-5023(05)80033-4.
- 13. Kauer JM. The articular disc of the hand. Acta Anat (Basel). 1975;93(4):590-605. doi: 10.1159/000144537.
- 14. Mohiuddin A, Janjua MZ. Form and function of the radioulnar articular disc. Hand. 1982;14(1):61-6. doi: 10.1016/s0072-968x(82)80044-2.
- 15. Garcia-Elias M, Domènech-Mateu JM. The articular disc of the wrist. Limits and relations. Acta Anat (Basel). 1987;128(1):51-4. doi: 10.1159/000146314.
- 16. Hogikyan JV, Louis DS. Embryologic development and variations in the anatomy of the ulnocarpal ligamentous

- complex. J Hand Surg Am. 1992;17(4):719-23. doi: 10.1016/0363-5023(92)90323-h.
- 17. Kirchberger MC, Unglaub F, Mühldorfer-Fodor M, Pillukat T, Hahn P, Müller LP, Spies CK. Update TFCC: histology and pathology, classification, examination and diagnostics. Arch Orthop Trauma Surg. 2015;135:427-37. doi: 10.1007/s00402-015-2153-6.
- 18. Semisch M, Hagert E, Garcia-Elias M, Lluch A, Rein S. Histological assessment of the triangular fibrocartilage complex. J Hand Surg Eur. 2016;41(5):527-33. doi: 10.1177/1753193415618391.
- 19. Bednar JM, Osterman AL. The role of arthroscopy in the treatment of traumatic triangular fibrocartilage injuries. Hand Clin. 1994;10(4):605-14.
- 20. Ohmori M, Azuma H. Morphology and distribution of nerve endings in the human triangular fibrocartilage complex. J Hand Surg Br. 1998;23(4):522-5. doi: 10.1016/s0266-7681(98)80137-x.
- Rein S, Semisch M, Garcia-Elias M, Lluch A, Zwipp H, Hagert E. Immunohistochemical Mapping of Sensory Nerve Endings in the Human Triangular Fibrocartilage Complex. Clin Orthop Relat Res. 2015;473(10):3245-53. doi: 10.1007/s11999-015-4357-z.
- 22. Palmer AK. Triangular fibrocartilage complex lesions: a classification. J Hand Surg Am. 1989;14(4):594-606. doi: 10.1016/0363-5023(89)90174-3.
- 23. Lawler E, Adams BD. Reconstruction for DRUJ instability. Hand (N Y). 2007;2(3):123-6. doi: 10.1007/s11552-007-9034-6.
- 24. Hagert E, Lalonde DH. Wide-Awake Wrist Arthroscopy and Open TFCC Repair. J Wrist Surg. 2012;1(1):55-60. doi: 10.1055/s-0032-1312045.
- 25. Sarkissian EJ, Burn MB, Yao J. Long-Term Outcomes of All-Arthroscopic Pre-Tied Suture Device Triangular Fibrocartilage Complex Repair. J Wrist Surg. 2019;8(5):403-407. doi: 10.1055/s-0039-1688949.
- Shigemitsu T, Tobe M, Mizutani K, Murakami K, Ishikawa Y, Sato F. Innervation of the triangular fibrocartilage complex of the human wrist: a quantitative immunohistochemical study. Anat Sci Int. 2007;82(3):127-32. doi: 10.1111/j.1447-073X.2007.00173.x.
- 27. Bednar JM, Osterman AL. The role of arthroscopy in the treatment of traumatic triangular fibrocartilage injuries. Hand Clin. 1994;10(4): 605-14.
- 28. Zhan H, Zhang H, Bai R, Qian Z, Liu Y, Zhang H, et al. High-resolution 3-T MRI of the triangular fibrocartilage complex in the wrist: injury pattern and MR features. Skeletal Radiol. 2017;46(12):1695-1706. doi: 10.1007/s00256-017-2739-x.
- 29. Atzei A, Luchetti R. Foveal TFCC tear classification and treatment. Hand Clin. 2011;27(3):263-72. doi: 10.1016/j.hcl.2011.05.014.